

Carrier Transport Mechanism of Copper Phthalocyanine Based Photodiode for Solar Cell Applications

T. Elmore¹, J. Candler¹, F. Yakuphanoglu² and R.K. Gupta^{1,*}

¹Department of Chemistry, Pittsburg State University, Pittsburg, KS 66762, USA

²Department of Physics, Faculty of Science, Firat University, Elazig 23169, Turkey

Abstract: Copper phthalocyanine (CuPc)/n-silicon junction was fabricated using thermal evaporator method. X-ray analysis of the CuPc film confirms the β -phase with preferred orientation along (100) direction. The crystallite size of the CuPc film was estimated using XRD data and observed to be about 12.6 nm. The current-voltage characteristics of Au/CuPc/n-Si/Au device was studied in dark and under illumination. The device showed diode characteristics. The diode parameters such as ideality factor, barrier height and series resistance were determined using different techniques such as conventional forward bias I-V characteristics, Cheung method and Norde's function. A good agreement between the diode parameters calculated from these methods was observed. The analysis of the diode characteristics confirmed that the transport mechanism of the Au/CuPc/n-Si/Au diode at the higher electric fields was governed by the space-charge-limited currents. The photoconducting behavior of the diode suggests that it can be used as a photosensor in optoelectronic applications.

Keywords: Copper phthalocyanine, Schottky diode, photodiode, I-V characteristics.

INTRODUCTION

Phthalocyanine compounds have attracted considerable attention because of their wide applications in organic light emitting diodes, field effect transistor, laser protection, molecular sensor, and solar cells [1-4]. Copper phthalocyanine (CuPc) is used as an active layer in these devices because of its low cost, low toxicity, high chemical stability and compatibility with flexible substrate [5, 6]. In addition, copper phthalocyanine could be grown as very thin films under ultra-high vacuum [7]. The properties and efficiency of the devices largely depend on the junction characteristics, therefore it is very important to understand the electronic properties at junction for CuPc.

Gorgoi and Zahn have studied the charge-transfer mechanism at silver/phthalocyanines interfaces [8]. A physisorption model for charge transport was reported based on the observation that a charge-transfer from Ag to CuPc occurs at the Ag/CuPc interface for thicker Ag layers but there was no sign of chemical interaction. A hysteresis and offset of current-voltage characteristics of diodes based on Ag/CuPc/ITO was reported [9]. Prabakaran *et al* [6] have fabricated a hybrid solar cell using CuPc and porous silicon. They used different volume fractions (52% and 62%) of porous Si crystalline for fabrication of a hybrid solar cell. It was observed that the porous silicon layer with a

more crystalline fraction was more appropriate for hybrid solar cell performances.

Junction properties of ITO/CuPc/Al diodes were studied at various temperatures [10]. It was observed that the charge-transport mechanism of the device largely depend on bias voltage and temperature. At low bias and high temperature, the charge transport follow the Poole-Frenkel type transport model, whereas at high bias and low temperature, space charge limited current controlled by an exponential distribution of traps was the dominating charge transport mechanism.

In present study, we have fabricated CuPc/n-silicon junction using thermal evaporator method. Current-voltage characteristics of the device was studied in dark and under illumination. Various junction parameters were calculated. The charge-transport mechanism of the device was proposed based on its current-voltage characteristics.

EXPERIMENTAL DETAILS

The copper phthalocyanine powder used in this study was obtained from Aldrich, USA. The CuPc film was deposited on n-silicon using thermal evaporator technique under high vacuum (1×10^{-6} mbar). The average rate of CuPc evaporation was 0.1 nm/s. Before CuPc deposition, the native oxide layer of the silicon substrate was etched using HF solution and then rinsed in deionised water using an ultrasonic bath for 10-15 min. Finally silicon wafer was chemically cleaned according to method based on successive baths of methanol and acetone. Top contact of the

*Address correspondence to this author at the Department of Chemistry, Pittsburg State University, Pittsburg, KS 66762, USA; Tel: +1 620 2354763; Fax: +1 620 2354003; E-mail: ramguptamsu@gmail.com

diodes was prepared by evaporating Au metal. The area of the Au contact was $3.14 \times 10^{-2} \text{ cm}^2$. The structural characterization was done using X-ray diffraction (XRD). The XRD spectra of the films were recorded with Bruker AXS x-ray diffractometer using the 2θ - θ scan with $\text{CuK}\alpha$. The optical transmittance measurements were made using UV-visible spectrophotometer (Ocean Optics HR4000). The current-voltage (I-V) characteristics of the diode were performed with KEITHLEY 4200 semiconductor characterization system. Photo dependence measurements were performed using a 200 W halogen lamp.

RESULTS AND DISCUSSIONS

The X-ray diffraction pattern of the as grown CuPc film is shown in Figure 1. It is well known that phthalocyanine materials can exist in several crystalline polymorphs, such as α , β , χ , and γ polymorphs [11]. The obtained XRD pattern of the CuPc film indicates β -form with preferred orientation along (100) plane. Rajesh *et al* [12] have observed similar behavior for vapor deposited CuPc film. The crystallite size (L) of the CuPc was estimated using Scherrer's formula:

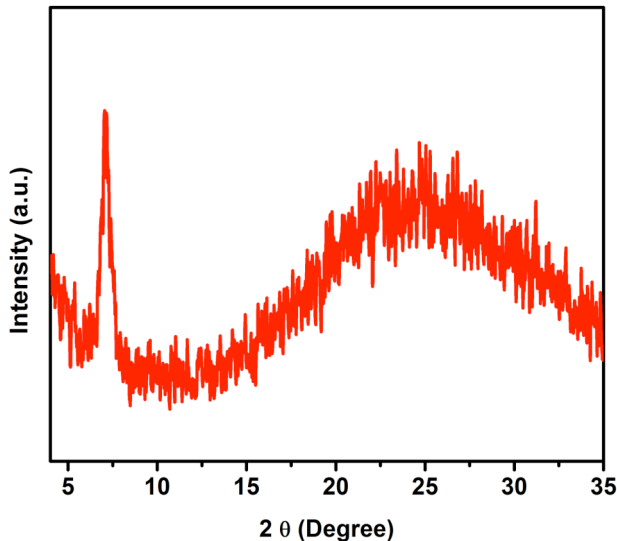


Figure 1: X-ray diffraction pattern of CuPc film.

$$L = \frac{0.9\lambda}{\beta_0 \cos \theta} \quad (1)$$

where λ is the wavelength of the X-ray, β_0 is the width at half maximum intensity in radians, θ is the Bragg's angle. The mean crystal size of the CuPc was estimated to be 12.6 nm. The optical absorbance and transmittance spectra of the CuPc film is shown in Figure 2. As seen in the transmittance spectra, CuPc shows B ($\pi \rightarrow \pi^*$) band around 450 nm and Q ($n \rightarrow \pi^*$)

band around 670 nm. Chiu *et al* [13] have observed similar absorption spectra for the physical vapor deposited CuPc films. The optical band gap of the film was calculated using the data of transmittance vs. wavelength plot. The absorption coefficient (α) was determined by equation $\alpha = \ln(1/T)/d$, where T is the transmittance and d is the film thickness. The band gap of film is determined by plotting $(\alpha h\nu)^2$ versus $h\nu$ [14]. Extrapolation of this plot to $\alpha^2 = 0$ gives the optical band gap energy of CuPc (Figure 3). The band gap of the CuPc was observed to be 1.77 eV. The obtained bandgap of CuPc is in good agreement with other reports [15, 16].

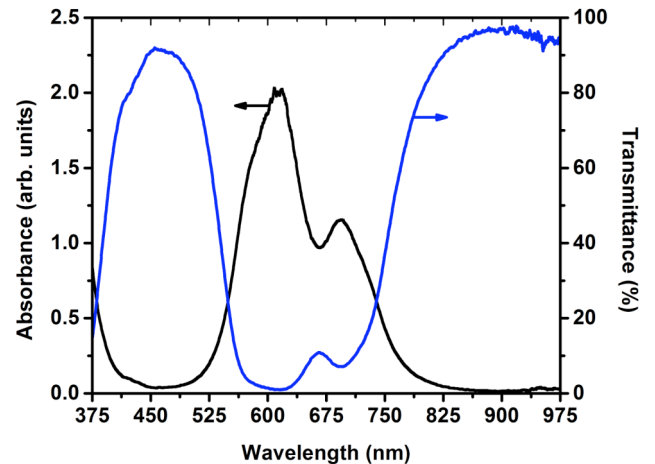


Figure 2: Optical absorbance and transmittance spectra of CuPc film.

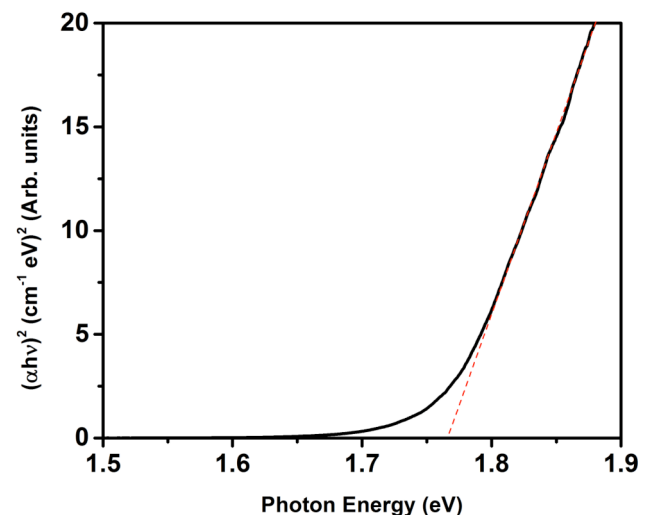


Figure 3: Photon energy dependence of $(\alpha h\nu)^2$ of CuPc film.

The current-voltage (I-V) characteristic of Au/CuPc/n-Si/Au device was studied in dark and under illumination. Figure 4 shows the I-V characteristics of the device under dark whereas Figure 5 and 6 shows the I-V characteristics of the device in dark and under

illumination. The inset of Figure 5 shows the schematic diagram of the device. The device clearly shows the non-linear behavior similar to diode. Such non-linear behavior could be analyzed using thermionic emission model. According to this model, the current of the diode could be expressed as [17]

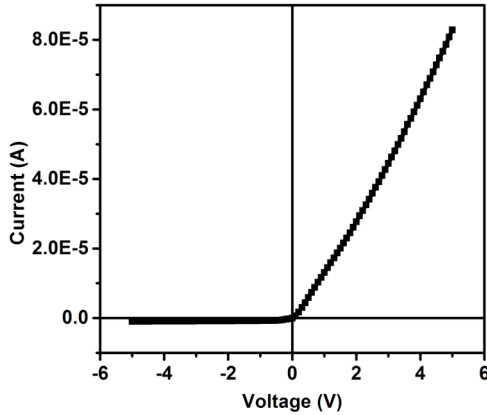


Figure 4: I-V characteristic of the Au/CuPc/n-Si/Au diode in dark.

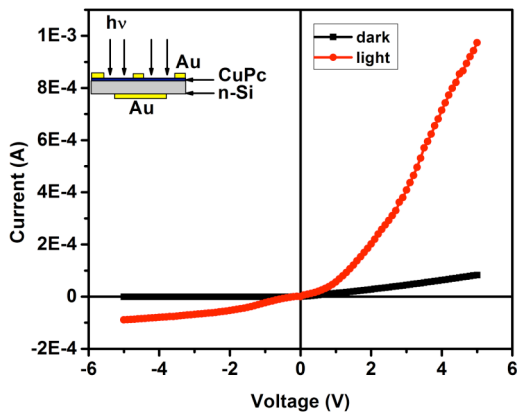
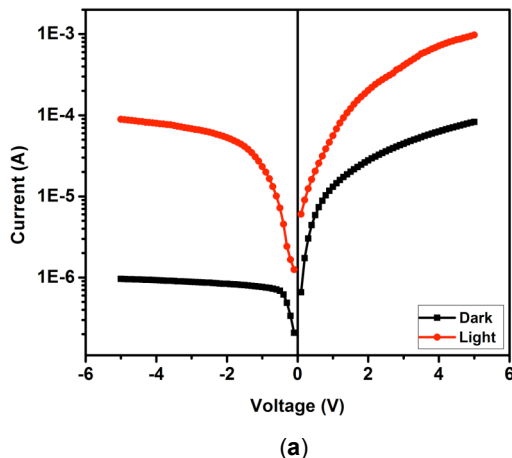
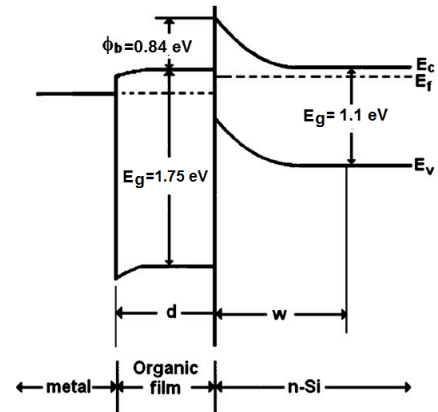


Figure 5: I-V characteristic of the Au/CuPc/n-Si/Au diode in dark and under illumination.



(a)



(b)

Figure 6: (a) logI-V characteristic of the Au/CuPc/n-Si/Au diode in dark and under illumination and (b) Energy band diagram of the diode.

$$I = I_0[\exp(qV/nkT) - 1] \quad (2)$$

where, I_0 is the saturation current, k is the Boltzmann constant, T is the absolute temperature, q is the elementary electric charge, V is applied voltage, and n is the ideality factor. The saturation current (I_0) is expressed as

$$I_0 = AA^* T^2 \exp(-q\phi_b/kT) \quad (3)$$

where, A is the active device area, A^* is the effective Richardson constant, and ϕ_b is the barrier height. The ideality factor and the barrier height of the device was determined from the expressions given below:

$$n = [q/kT] \cdot [dV/d(\ln I)] \quad (4)$$

$$\phi_b = kT/q \ln(AA^* T^2 / I_0) \quad (5)$$

The ideality factor and the barrier height of the diode was estimated to be 4.62 and 0.48 eV. The higher ideality value could be due to presence of native oxide layer on the silicon substrate, accelerated recombination of electrons and holes in the depletion region, the presence of interfacial layer, and the presence of imperfections [17-20]. The ideality factor of 3.02 and barrier height of 0.84 eV was reported for FTO/CuPc/Al Schottky device [12].

The energy band diagram and structure of Au/CuPc/n-Si/Au diode is shown in Figure 6b, in which, E_f is the Fermi level, d is the thickness of organic layer, ϕ_b is the barrier height, E_g is the band gap of the semiconductors, and w is the width of the depletion region. In order to analyze the contribution of high electric fields to I-V characteristics of the Au/CuPc/n-Si/Au diode, the forward bias I-V characteristics were plotted in double logarithmic scale, as shown in Figure 7. As

seen in Figure 7, the plot exhibits two linear regions. The lower potential region (I) shows a slope of 1.39, whereas as the higher potential region shows a slope of 1.07. The power law behavior observed in the $\log(I)$ - $\log(V)$ plot indicates that charge transport of the diode is influenced by space-charge-limited current (SCLC) process. Huang *et al* [21] have also observed two linear regions in the $\log(I)$ - $\log(V)$ plot of the Au/CuPc/Al Schottky diode. The first region showed a slope of 1.9 and second region showed a slope of 5. For the Au/p-ZnPc/p-Si diode, only one linear region with a slope of 2 was reported [22]. The SCLC process occurs only when the injecting electrode is an Ohmic contact, and therefore a reservoir of charge is presented. When an Ohmic contact is applied, majority carriers could be injected into the CuPc film, and when the injected carrier concentration exceeds the thermally generated concentration, the SCLC becomes dominant. The observed higher ideality factor could be due to presence of series resistance across the junction. The series resistance of the junction is determined from the forward bias I-V characteristics. According to Chenug and Cheung methods, the forward bias I-V characteristic of a device having series resistance is expressed by the following relation [23]

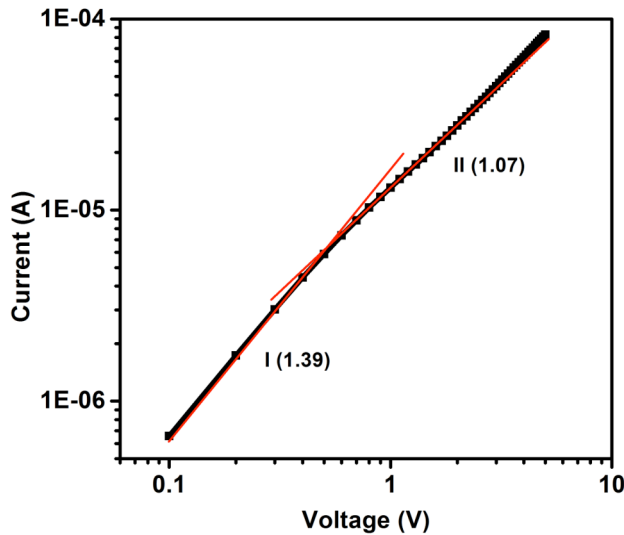


Figure 7: The forward bias $\log(I)$ - $\log(V)$ plot of Au/CuPc/n-Si/Au diode.

$$I = I_0 \exp[q(V - IR_s)/nkT] \quad (6)$$

where, the IR_s is the voltage drop across the series resistance of device. The value of series resistance is determined by the following equation

$$H(I) = n\phi_b + IR_s \quad (7)$$

$$\text{where, } H(I) = V - (nkT/q) \ln(I/AA^*T^2) \quad (8)$$

Series resistance for the diode was calculated using equation (7). A plot of $H(I)$ versus I will linear, the slope of this plot gives a value of series resistance (Figure 8). The value of series resistance of the diode was calculated as 6.3 k Ω . The series resistance of the diode was also calculated using Norde's method for comparison [24]. In Norde model, the Norde functions can be given by the following relation,

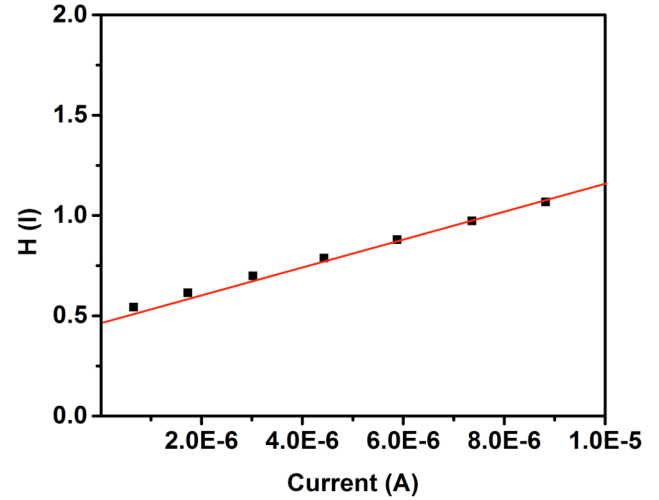


Figure 8: The forward bias $H(I)$ - I plot of Au/CuPc/n-Si/Au diode.

$$F(V) = V/\gamma - (kT/q) \ln[I(V)/AA^*T^2] \quad (9)$$

where, γ is the integer (dimensionless) greater than n . The minimum of the F vs. V plot was used to determine the series resistance. Figure 9 shows the $F(V)$ vs. V plot of the Au/CuPc/n-Si/Au diode. The value of series resistance of the device was calculated using the equation given below

$$R_s = kT(\gamma - n)/qI \quad (10)$$

The value of the series resistance was found to be 5.7 k Ω . It is seen that the R_s resistance values obtained from Cheung and Norde methods are in agreement with each other. The obtained R_s value is higher and this causes non-linear I-V characteristics of the diode, in which the ideality factor is deviated from ideal value.

CONCLUSION

A photodiode using CuPc was fabricated using thermal evaporator method. The as deposited CuPc film shows preferred orientation along (100) direction. The detailed current-voltage characteristics of the diode was studied under dark and light. It was observed that the current-voltage characteristics of the device is sensitive to light. The charge transport mechanism of the device was investigated. It was

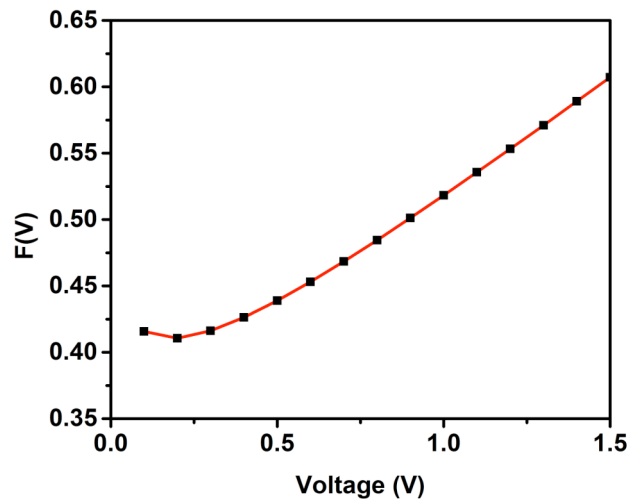


Figure 9: $F(V)$ - V plot of Au/CuPc/n-Si/Au diode.

found that at the higher electric fields, the charge transport mechanism is governed by space-charge-limited currents. The junction parameters such as ideality factor, barrier height and series resistance were calculated. The obtained results indicate that Au/CuPc/n-Si/Au diode can be used as a photosensor in optoelectronic applications.

ACKNOWLEDGEMENTS

Authors wish to thank Pittsburg State University for providing financial support. This material is based upon work supported by the National Science Foundation under Award No. EPS-0903806 and matching support from the State of Kansas through the Kansas Board of Regents.

REFERENCES

- [1] Kudo K, Iizuka M, Kuniyoshi S, Tanaka K. Device characteristics of lateral and vertical type organic field effect transistors. *Thin Solid Films* 2001 8/11; 393(1-2): 362-7.
- [2] Li F, Zheng Q, Yang G, Dai N, Lu P. Spectrum of copper phthalocyanine: Experiments and semi-empirical quantum chemical calculations. *Physica B: Condensed Matter* 2008 5/11; 403(10-11): 1704-7.
- [3] Pizzini S, Timo GL, Beghi M, Butta N, Mari CM, Faltenmaier J. Influence of the structure and morphology on the sensitivity to nitrogen oxides of phthalocyanine thin-film resistivity sensors. *Sensors and Actuators* 1989 5/17; 17(3-4): 481-91.
- [4] Rostalski J, Meissner D. Monochromatic versus solar efficiencies of organic solar cells. *Sol Energy Mater Sol Cells* 2000 2/15; 61(1): 87-95.
- [5] Joseph CM, Menon CS. Device preparation and characteristics of CuPc transistor. *Mater Lett* 2002 1//; 52(3): 220-2.
- [6] Prabakaran R, Fortunato E, Martins R, Ferreira I. Fabrication and characterization of hybrid solar cells based on copper phthalocyanine/porous silicon. *J Non-Cryst Solids* 2008 5/1; 354(19-25): 2892-6.
- [7] Aristov VY, Molodtsova OV, Maslyuk V, Vyalikh DV, Zhilin VM, Ossipyan YA, et al. Electronic structure of pristine CuPc: Experiment and calculations. *Appl Surf Sci* 2007 10/31; 254(1): 20-5.
- [8] Gorgoi M, Zahn DRT. Charge-transfer at silver/phthalocyanines interfaces. *Appl Surf Sci* 2006 5/30; 252(15): 5453-6.
- [9] Thurzo I, Pham G, Zahn DRT. On the mechanism of the hysteresis and offset of current-voltage characteristics of diodes based on organic materials. *Chem Phys* 2003 2/1; 287(1-2): 43-54.
- [10] Reis FT, Mencaraglia D, Ould Saad S, Séguy I, Oukachmih M, Jolinat P, et al. Electrical characterization of ITO/CuPc/Al diodes using temperature dependent capacitance spectroscopy and I-V measurements. *J Non-Cryst Solids* 2004 6/15; 338-340(0): 599-602.
- [11] Berger O, Fischer WJ, Adolphi B, Tierbach S, Melev V, Schreiber J. Studies on phase transformations of Cu-phthalocyanine thin films. *J Mater Sci: Mater Electron* 2000 2000/06/01; 11(4): 331-46. English.
- [12] Rajesh KR, Varghese S, Menon CS. Determination of electrical and solar cell parameters of FTO/CuPc/Al Schottky devices. *J Phys Chem Solids* 2007 4//; 68(4): 556-60.
- [13] Chiu K-C, Juey L-T, Su C-F, Tang S-J, Jong M-N, Wang S-S, et al. Effects of source and substrate temperatures on the properties of ITO/CuPc/C60 heterostructure prepared by physical vapor deposition. *J Cryst Growth* 2008 4//; 310(7-9): 1734-8.
- [14] Marotti RE, Guerra DN, Bello C, Machado G, Dalchiele EA. Bandgap energy tuning of electrochemically grown ZnO thin films by thickness and electrodeposition potential. *Sol Energy Mater Sol Cells* 2004 5/1; 82(1-2): 85-103.
- [15] Pirriera MD, Puigdollers J, Voz C, Stella M, Bertomeu J, Alcubilla R. Optoelectronic properties of CuPc thin films deposited at different substrate temperatures. *J Phys D: Appl Phys* 2009; 42(14): 145102. <http://dx.doi.org/10.1088/0022-3727/42/14/145102>
- [16] Sueyoshi T, Kakuta H, Ono M, Sakamoto K, Kera S, Ueno N. Band gap states of copper phthalocyanine thin films induced by nitrogen exposure. *Appl Phys Lett* 2010; 96(9): 093303. <http://dx.doi.org/10.1063/1.3332577>
- [17] Rhoderick EH, Williams RH. *Metal-Semiconductor Contacts*: Clarendon Press, Oxford 1988; 1988.
- [18] Sze S. *Physics of semiconductor devices* 1979: New York, Wiley.
- [19] Gupta RK, Yakuphanoglu F. Analysis of device parameters of Al/In2O3/p-Si Schottky diode. *Microelectron Eng* 2013 5//; 105(0): 13-7.

- [20] Reddy VR, Reddy MSP, Lakshmi BP, Kumar AA. Electrical characterization of Au/n-GaN metal–semiconductor and Au/SiO₂/n-GaN metal–insulator–semiconductor structures. *J Alloys Compd* 2011; 509(31): 8001-7.
<http://dx.doi.org/10.1016/j.jallcom.2011.05.055>
- [21] Huang C-Y, Lin S-Y, Cheng S-S, Chou S-T, Yang C-Y, Ou T-M, *et al.* Transport mechanisms and the effects of organic layer thickness on the performance of organic Schottky diodes. *Journal of Vacuum Science & Technology B* 2007; 25(1): 43-6.
<http://dx.doi.org/10.1116/1.2404682>
- [22] El-Nahass MM, Zeyada HM, Aziz MS, El-Ghamaz NA. Carrier transport mechanisms and photovoltaic properties of Au/p-ZnPc/p-Si solar cell. *Solid-State Electron* 2005 8//; 49(8): 1314-9.
- [23] Cheung SK, Cheung NW. Extraction of Schottky diode parameters from forward current-voltage characteristics. *Appl Phys Lett* 1986; 49(2): 85-7.
<http://dx.doi.org/10.1063/1.97359>
- [24] Norde H. A modified forward I-V plot for Schottky diodes with high series resistance. *J Appl Phys* 1979; 50(7): 5052-3.
<http://dx.doi.org/10.1063/1.325607>

Received on 23-02-2015

Accepted on 23-03-2015

Published on 15-04-2015

DOI: <http://dx.doi.org/10.15377/2410-2199.2015.02.01.4>© 2015 Elmore *et al.*; Avanti Publishers.

This is an open access article licensed under the terms of the Creative Commons Attribution Non-Commercial License (<http://creativecommons.org/licenses/by-nc/3.0/>) which permits unrestricted, non-commercial use, distribution and reproduction in any medium, provided the work is properly cited.